Cobalt-tetraphenylporphyrin-based hypercrosslinked polymer for efficient CO_2 photoreduction to CO

Saif Ullah,[a] Xunliang Hu,[a] Yaqin Zhang,[a] Irshad Hussain,[b] Xiaoyan Wang,[a] Hui Gao*[a] and Bien Tan*[a]

a. Key Laboratory of Material Chemistry for Energy Conversion and Storage Ministry of Education, Hubei Key Laboratory of Material Chemistry and Service Failure, School of Chemistry and Chemical Engineering, Huazhong University of Science and Technology, Luoyu Road No. 1037, 430074 Wuhan, P. R. China.

b. Department of Chemistry & Chemical Engineering, SBA School of Science & Engineering, Lahore University of Management Sciences (LUMS), DHA, Lahore Cantt, Lahore 54792, Pakistan

E-mail: bien.tan@mail.hust.edu.cn

1. Experimental Section

1.1 Material

Cobalt acetate ($Co(OAc)_2.4H_2O$, 99.99%), tetrahydrofuran (THF, 99.5%), and 5, 10, 15, 20-tetraphenylporphyrin (TPP, 97%) were brought from Aladdin Chemical Reagents Corp. (Shanghai, China). Dichloromethane (DCM, 99.5%), anhydrous aluminum chloride ($AlCl_3$, 98.5%), methanol (MeOH, 99.7%), ethanol (EtOH, 99.7%), and hydrochloric acid (HCl, 36.0~38.0%) were purchased from Sinopharm Chemical Reagent Co., Ltd (Shanghai, China). All the chemicals were used without further purification. 18.2 MΩ of resistivity deionized water was produced on-site.

1.2 Synthesis Procedure

Synthesis of tetraphenyl porphyrin base polymer (HCP-TPP)

To synthesize hyper crosslinked tetraphenyl porphyrin (HCP-TPP), a controlled chemical process is conducted under a nitrogen atmosphere. Initially, tetraphenyl porphyrin (TPP, 1.9 mmol, 1.2 g) is dispersed in dichloromethane (16 mL), followed by the addition of aluminum chloride as a catalyst ($AlCl_3$, 31.7 mmol, 4.23 g). At progressively increasing temperatures from 0 °C for 6 hours, 30 °C for 8 hours, 40 °C for 12 hours, 60 °C for 12 hours, and 80 °C for 24 hours, this mixture is constantly stirred for 62 hours. After that, the temperature gradually drops to room temperature. Following the reaction process, a HCl-H_2O (2/1=v/v) solution is used to quench the mixture and stopping the reaction. This solid is then subjected to multiple washings with water and ethanol. A further purification step contains ethanol extraction using a Soxhlet apparatus. The final step involves drying the product in a vacuum oven at 100 °C for 24 hours. The obtained product is black solid powder, with a yield of 170 %.

Polymer yield calculation

$$Yield = \frac{m_{polymer}}{m_{monomer}} \times 100\%$$

$m_{polymers}$ is quantity of dry polymers prepared through solvent knitting strategy, $m_{monomers}$ is the quantity of consistent monomers of the polymers.[1-3]

Synthesis of Cobalt anchored into tetraphenylporphyrin-based polymer (HCP- CoTPP)

To synthesize the HCP-CoTPP, the process begins with HCP-TPP (200 mg) is suspended in tetrahydrofuran (20 mL) and stirred for several hours. The mixture is supplemented with cobalt acetate (80 mg) and heated to 80 °C for 24 hours under continuous stirring in a nitrogen atmosphere.

After the reaction, the resultant solid is separated from the mixture and subjected to extensive washing with both ethanol and water, then Soxhlet extracted for 48 hours with ethanol for further purification. The product was dried at 60 °C in a vacuum oven for 24 h.

1.3 Characterization

Fourier Transform Infrared (FT-IR) spectra were acquired at room temperature and air pressure using the KBr pellet method with a Bruker VERTEX 70 FTIR spectrometer. Solid-state ^{13}C Cross-Polarizaton/Magic Angle Spinning (CP/MAS) Nuclear Magnetic Resonance (NMR) spectra were acquired using a Bruker Avance II WB 400 MHz spectrometer, equipped with a 4 mm double-resonance MAS probe, spinning at 8 kHz. The polymer morphologies were observed using an FEI Sirion 200 field-emission scanning electron microscope (FE-SEM) at a voltage of 10 kV acceleration. To get ready for these microscopy experiments, the materials were dried for 24 hours at 70 °C in a vacuum oven. After the samples was dried, platinum was sputtered onto the samples to increase electron conductivity. Co content data was collected using an Agilent Corp., USA, ICP-OES 730 equipment outfitted with an Inductively Coupled Plasma Optical Emission Spectrometer (ICP-OES) system. Thermogravimetric analysis (TGA) was carried out using a PerkinElmer Pyris 1 TGA system with a continuous nitrogen flow. By maintaining a constant rate of 10 °C per minute, the surrounding temperature rose to 850 °C. The X-ray photoelectron spectroscopy (XPS) measurement were taken by Kratos AXIS-ULTRA DLD-600 was used to measure the spectra. The specific surface area of several samples as well as the sorption properties of gases, namely nitrogen (N_2) and carbon dioxide (CO_2), were evaluated using a Micromeritics ASAP 2460 surface area and porosity analyzer. To ensure that any contaminants that had adsorbed were eliminated, the samples were degassed for eight hours at 110 °C and 10-5 bar of lower pressure prior to analysis. Based on the nitrogen adsorption isotherm data and the assumption of slit-pore geometry, the pore size distribution inside the samples was ascertained using the Tarazona non-local density functional theory (NLDFT) model. The total pore volume (V_{total}) of the samples was considered using the nitrogen adsorption isotherm at a relative pressure (P/P_0) of 0.995.

1.4 Catalysis Protocol

Carbon Dioxide Reduction Experiments: Acetonitrile, water, triethanolamine (TEOA) (3:1:1 vol. combination, 10 mL), catalyst (2 mg), and $[Ru(Bpy)_3Cl_2]$ (2 mg) were added to a quartz flask

before it was sealed. After being ultrasonicated for 15 minutes, the suspension was purged with gaseous CO_2 for 20 minutes. The reaction mixture was exposed to radiation for the experimental method using a 300 W Xenon lamp fitted with a filter that allowed $\lambda \geq 420$ nm. After the gas was exposed to radiation, it was collected using a gas-tight syringe and its composition was examined using a Shimadzu GC-2014 gas chromatograph.

Isotope-labelling experiment process

In quartz flask, HCP-CoTPP (2 mg), $[Ru(Bpy)_3Cl_2]$ (2 mg) was added to a solvent mixture of acetonitrile, water, and triethanolamine (3:1:1= 10 mL). The flask was then sealed with a septum. The mixture was sonicated for 5 minutes, then purged with $^{13}CO_2$ for 5 minutes. The reaction mixture was then exposed to 300 W Xe light source (fitted with the cut-of filter of $\lambda \geq 420$ nm) for 4 hours. The gas-phase analysis was conducted using gas chromatography (Agilent GC-MS 7890B) coupled with a mass spectrometer (Agilent GC-MS 5977B) through a GCOCARBONPLOT column, which is 60 meters long with a 0.32 mm inner diameter.

Apparent quantum yield (AQY) calculation

In a quartz flask, 2 mg of HCP-CoTPP and 2 mg of $[Ru(Bpy)_3Cl_2]$ were added in a solvent mixture of acetonitrile, water, and triethanolamine (TEOA) at a volumetric ratio of 3:1:1. The total volume of the solution was adjusted to 10 mL. This flask was then tightly sealed to prevent any gas exchange with the environment. Then, the mixture subjected ultrasonication for 10 min, a step essential for ensuring a homogeneous dispersion of the catalysts within the solvent medium. Subsequently, the resultant suspension was subjected to a CO_2 purging process for 20 min, aimed at saturating the reaction medium with CO_2, thereby facilitating the photocatalytic reduction process.

A 300 W Xenon lamp equipped with selective bandpass filters illuminated the mixture, targeting specific wavelengths of 420 nm, 450 nm, 500 nm, and 550 nm. The resultant illumination intensities for these wavelengths were documented at 20.0 mW cm^{-2} for 420 nm, 16.6 mW cm^{-2} for 450 nm, 21.4 mW cm^{-2} for 500 nm, and 21.0 mW cm^{-2} for 550 nm. By employing a cooling water flow, the reaction system's temperature was kept constant at 25 °C. Using the matching equation, the AQY at a certain light irradiation wavelength was determined.

$$AQY\ (\%) = \frac{2CN_A}{SPt\lambda/hc} \times 100$$

The given context, "h" represents Planck's constant, valued at (6.626×10^{34} J s) a fundamental constant used in quantum mechanics. "S" refers to the surface area of the bandpass filter, measured

to be 19.63 cm^2. The variable "C" denotes the quantity of carbon monoxide (CO) generated, expressed in milligrams per hour. "N_A" stands for Avogadro's constant, which is 6.02×10^{23} molecules mol^{-1}. "t" indicates the duration of light exposure, set at 3600 seconds (equivalent to one hour), and "P" symbolizes the specific light intensity impacting the sample (W cm^{-2}).

2. Supplementary data

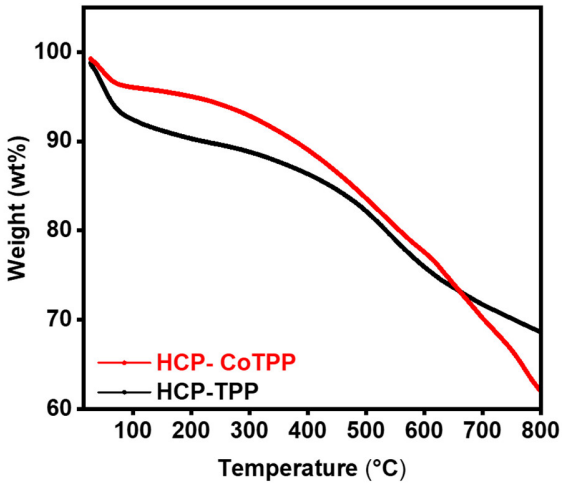

Fig. S1. TGA of the HCP-TPP and HCP-CoTPP with a heating rate of 10 ℃ min^{-1} under N_2 environment

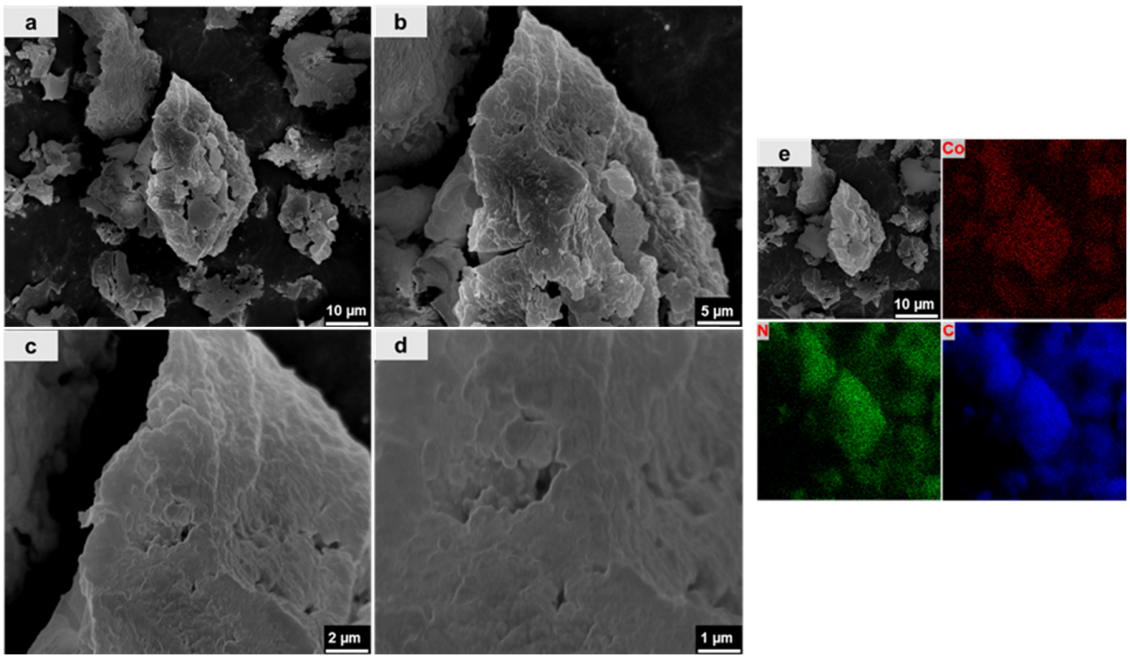

Fig. S2. (a-d) FE-SEM image of HCP-CoTPP and (e) EDX mapping of HCP-CoTPP. Scale bar: (a) 10 µm, (b) 5 µm, (c) 2 µm, (d) 1 µm, (e) 10 µm.

The composition of HCP-CoTPP was analyzed using energy-dispersive X-ray spectroscopy (EDX). Elements C, N and Co were confirmed by EDX analysis, and elemental mapping demonstrated a homogeneous distribution of the elements in the polymer matrix (Figure S2).

Table S1. Porosity properties of HCPs.

Polymer	S_{BET}[a] ($m^2\ g^{-1}$)	S_{Lang}[b] ($m^2\ g^{-1}$)	M_{PV}[c] ($cm^3\ g^{-1}$)	PV[d] ($cm^3\ g^{-1}$)
HCP-TPP	1239	1974	0.29	0.76
HCP-CoTPP	861	1208	0.23	0.47

[a]Surface area calculated from the nitrogen adsorption isotherm at 77.3 K using the BET equation. [b]Micropore surface area calculated from the nitrogen adsorption isotherm at 77.3 K using the *t*-plot equation. [c]Micropore volume calculated from the nitrogen isotherm at P/P_0 = 0.15, 77.3 K using the *t*-plot equation. [d]Pore volume calculated from the nitrogen isotherm at P/P_0 = 0.99, 77.3 K.

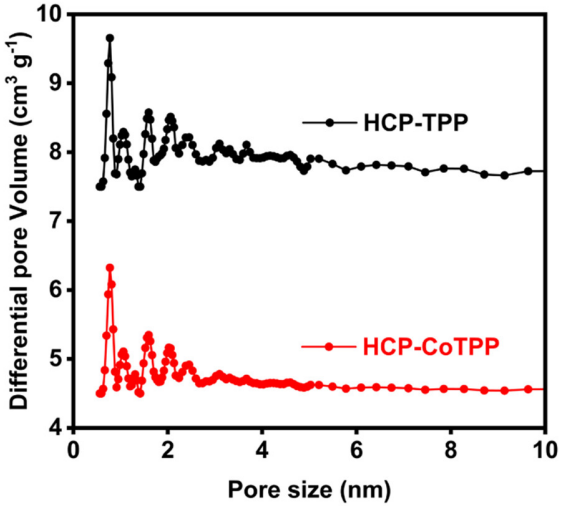

Fig. S3. Pore size distribution of HCP-TPP and HCP-CoTPP (measured through DFT method).

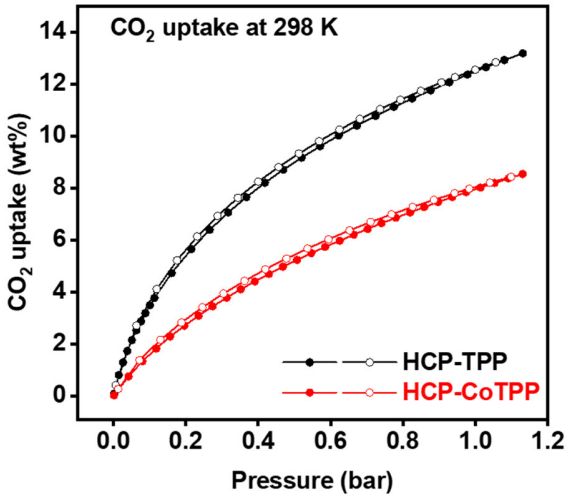

Fig. S4. CO_2 adsorption-desorption isotherm of HCPs at 298 K.

Table S2: CO_2 sorption properties of polymers

Polymer	CO_2 uptake [a] wt %	CO_2 uptake [b] wt %	Q_{st}[c] KJ mol^{-1}
HCP-TPP	21.9	13.5	29.2
HCP-CoTPP	13.1	8.2	31.2

[a]Volumetric CO_2 uptake measured with a Micromeritics ASAP 2020 M analyzer at 1.13 bar and 273 K.

[b]Volumetric CO_2 uptake measured with a Micromeritics ASAP 2020 M analyzer at 1.13 bar and 298 K.

[c]Isosteric heat of adsorption of polymers determined volumetrically using a Micromeritics ASAP 2020 M analyzer at273 and 298 K.

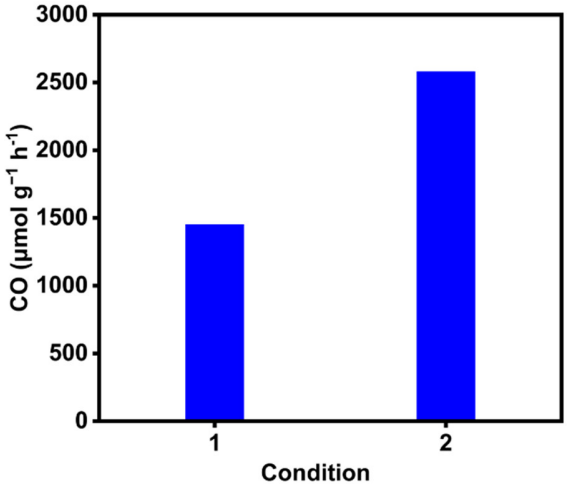

Fig. S5. Photocatalytic CO_2 conversion rate were measured under two different condition using HCP-CoTPP (2 mg) as catalyst and $[Ru(Bpy)_3]Cl_2$= (2 mg) under visible light irradiation ($\lambda \geq 420$ nm). Condition 1: Solvent mixture of MeCN, H_2O, and TEOA (3:1:1= 10 mL). Condition 2: Solvent mixture of DMF, H_2O, and TEOA (3:1:1= 10 mL).

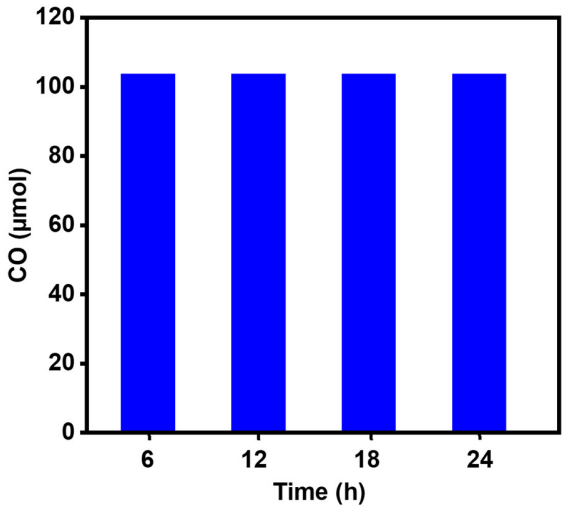

Fig. S6. Recyclability test under visible light irradiance using HCP-CoTPP (10 mg) with the presence of $[Ru(Bpy)_3]Cl_2$= (10 mg).

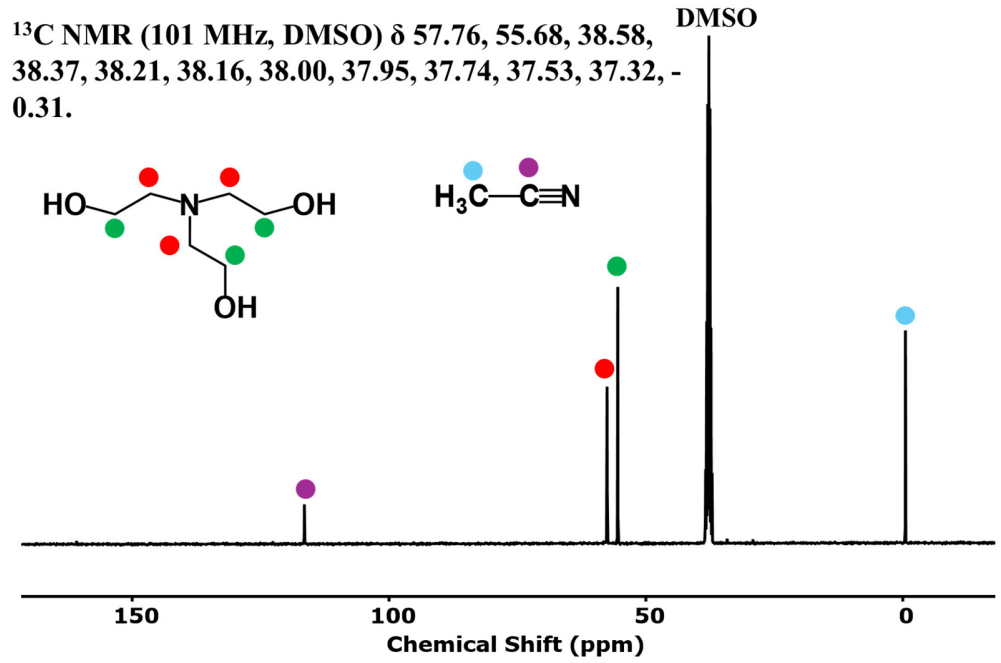

Fig. S7. ^{13}C NMR spectra of the solution after photocatalytic CO_2 reduction.

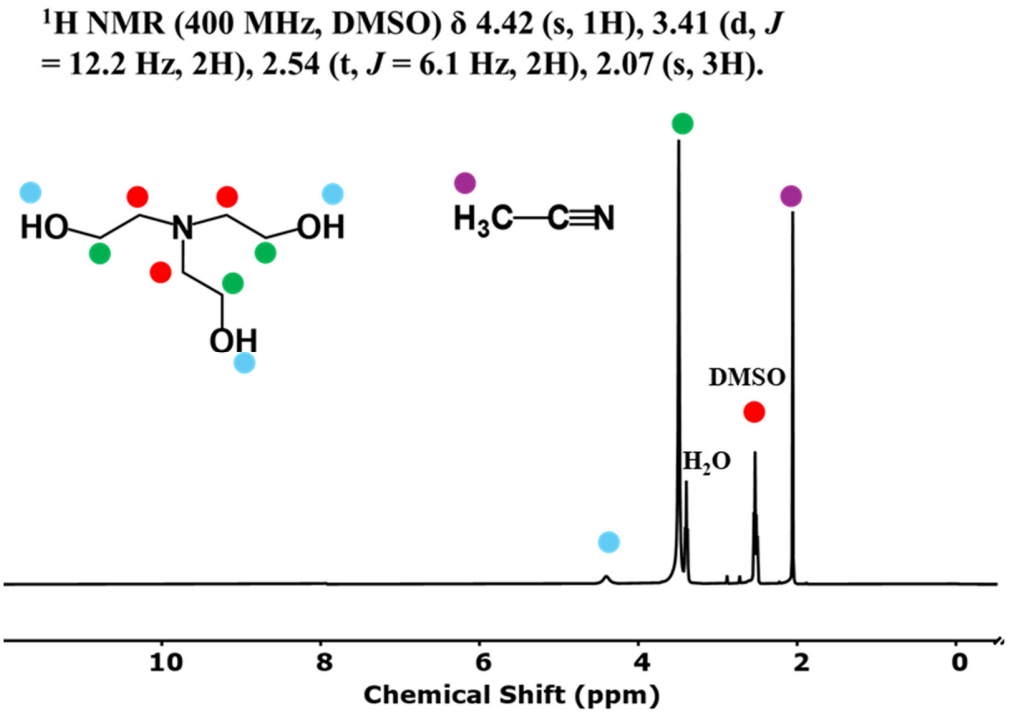

Fig. S8. ^{1}H NMR spectra of the solution after photocatalytic CO_2 reduction.

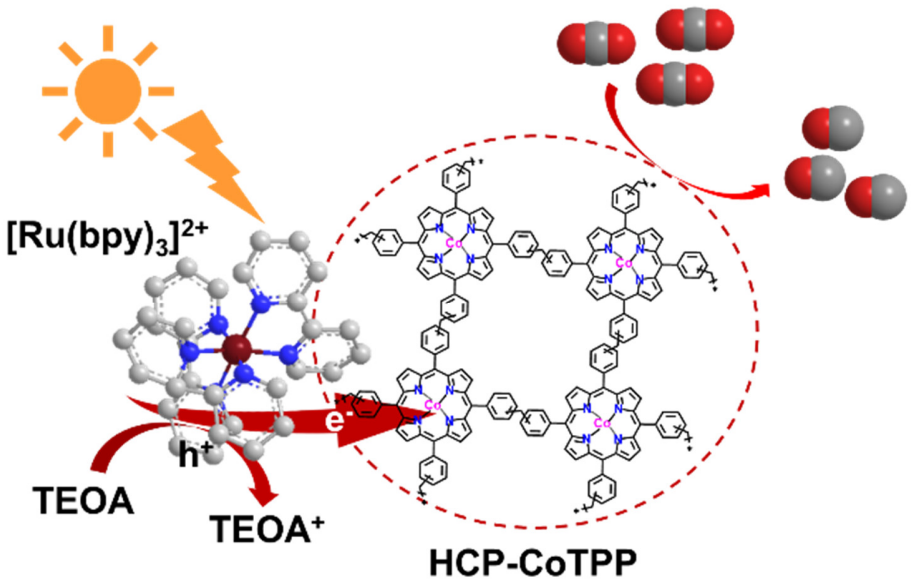

Fig. S9. Proposed reaction mechanism for the photocatalytic of CO_2 over HCP-CoTPP.

Table S3. Photocatalytic CO_2 reduction with various catalysts.

Photocatalyst	**Main product and highest yield ($\mu mol\ g^{-1}\ h^{-1}$)**	**Electron donor**	**Selectivity**	**Irradiation condition**	**Ref.**
HCP-CoTPP $[Ru(bpy)_3]Cl_2$	1449.9 (CO)	TEOA	100	$\lambda \geq 420$ nm (300 W Xe Light source)	**This work**
GO-COF-366-Co $[Ru(phen)_3](PF_6)_2$	52200 (CO)	TEOA	96.1	$\lambda > 320$ nm (300 W Xe lamp irradiation)	4
N-rich POP $[Ru(bpy)_3]Cl_2$	8 (Formic Acid)	TEOA	-	$\lambda \geq 420$ nm (300 W Xe lamp)	5
Fe^{II}/Fe^{III} MOF $[Ru(bpy)_3]Cl_2$	12270 (CO)	TEOA	90.6	$\lambda \geq 420$ nm (300 W Xenon lamp)	6
ImI-CMP@Co $[Ru(bpy)_3]Cl_2$	2953 (CO)	TEOA	90	$\lambda > 420$ nm (300 W Xe lamp)	7

Ni-TpBpy $[Ru(bpy)_3]Cl_2$	966 (CO)	TEOA	96	$\lambda \geq 420$ nm (300 W Xe)	8
NiP-TPE-COF $[Ru(bpy)_3]Cl_2$	525 (CO)	TEOA	93	$\lambda \geq 420$ nm (300 W Xe lamp)	9
NiPCD@TD-COF $[Ru(bpy)_3]Cl_2$	480 (CO)	TEOA	98	$\lambda \geq 420$ nm (Xe lamp)	10
POP2-Fe $[Ru(bpy)_3]Cl_2$	3043 (CO)	TEOA	90	500 W long-arc xenon lamp	11
H-COF-Ni $[Ru(bpy)_3]Cl_2$	1958 (CO)	TEOA	97	$\lambda \geq 420$ nm (Xe lamp)	12
Zn@BP-POP	215 (CO)	H_2O	94	$\lambda \geq 420$ nm (300 W Xe lamp)	13
TEB-GFP CMP	1666 (CO)	TEA	54	400−750 nm (300 W Xe lamp)	14
Amide-COP	20.6 (CO)	H_2O	-	λ>420 nm (300 W Xe lamp)	15
SO-TPB	40.12 (CO)	H_2O	100	λ >420 nm (300 W Xe)	16
HAzo-COPFs	53.6 (CO)	H_2O	99	$\lambda \geq 420$ nm (300 W Xe lamp)	17
Re@TEB-BPY	91.7 (CO)	TEA	68	400–750 nm (300 W xenon lamp)	18
Tx-TzTz-CMP-2	300.6 (CH_4)	H_2O	71.2	60 W LED	19

Re-TpBpy COF	275 (CO)	TEOA	96	$\lambda > 420$ nm (300 W Xe light source)	[20]
MOF-525-Co	200.6 (CO)	TEOA	97	$\lambda \geq 420$ nm (300 W xenon arc lamp)	[21]
Re-COF	750 (CO)	TEOA	81	200 to 1100 nm (300 W Xe lamp)	[22]
CPOP-30-Re	2414 (CO)	TEOA	61	300 W Xenon light	[23]
PI-COF	483 (CO)	TEOA	98	$\lambda \geq 420$ nm (300 W Xe lamp)	[24]
Metalated-POPs	145.6 (CO)	TEOA	93	$\lambda > 400$ nm (450 W xenon lamp)	[25]

Reference

1. J. S. M. Lee, M. E. Briggs, T. Hasell and A. I. Cooper, *Advanced Materials*, 2016, **28**, 9804-9810.
2. J. Hu, S. Yang, X. Wang, D. Zhang and B. Tan, *Macromolecules*, 2024.
3. Y. Cheng, S. Razzaque, Z. Zhan and B. Tan, *Chemical Engineering Journal*, 2021, **426**, 130731.
4. Y. N. Gong, J. H. Mei, W. J. Shi, J. W. Liu, D. C. Zhong and T. B. Lu, *Angewandte Chemie International Edition*, 2024, **63**, e202318735.
5. R. Newar, A. C. Ghosh, R. Kumari Riddhi, R. Rajapaksha, P. Samanta, F. M. Wisser and J. Canivet, *Advanced Energy and Sustainability Research*, 2024, **5**, 2300209.
6. Y. Zheng, X. Shen, M. Lin, M. Zhu, B. Yang, J. Yan, Z. Zhuang and Y. Yu, *Small*, 2024, **20**, 2306836.
7. W. Zhao, D. Zhai, C. Liu, D. Zheng, H. Wu, L. Sun, Z. Li, T. Yu, W. Zhou and X. Fang, *Applied Catalysis B: Environmental*, 2022, **300**, 120719.
8. W. Zhong, R. Sa, L. Li, Y. He, L. Li, J. Bi, Z. Zhuang, Y. Yu and Z. Zou, *Journal of the American Chemical Society*, 2019, **141**, 7615-7621.
9. H. Lv, R. Sa, P. Li, D. Yuan, X. Wang and R. Wang, *Science China Chemistry*, 2020, **63**, 1289-1294.
10. H. Zhong, R. Sa, H. Lv, S. Yang, D. Yuan, X. Wang and R. Wang, *Advanced Functional Materials*, 2020, **30**, 2002654.
11. X. Yao, K. Chen, L.-Q. Qiu, Z.-W. Yang and L.-N. He, *Chemistry of Materials*, 2021, **33**, 8863-8872.
12. S. Yang, R. Sa, H. Zhong, H. Lv, D. Yuan and R. Wang, *Advanced Functional Materials*, 2022, **32**, 2110694.
13. A. Boruah, B. Boro, R. Paul, C.-C. Chang, S. Mandal, A. Shrotri, C.-W. Pao, B. K. Mai and J. Mondal, *ACS Applied Materials & Interfaces*, 2024, **16**, 34437-34449.
14. F. A. Rahimi, A. Singh, R. Jena, A. Dey and T. K. Maji, *ACS Applied Materials & Interfaces*, 2024.
15. F. Wen, F. Zhang, Z. Wang, X. Yu, G. Ji, D. Li, S. Tong, Y. Wang, B. Han and Z. Liu, *Chemical Science*, 2021, **12**, 11548-11553.
16. C. Dai, L. Zhong, W. Wu, C. Zeng, Y. Deng and S. Li, *Solar RRL*, 2022, **6**, 2100872.

17. G. Ji, Y. Wang, W. Ye, M. Chen, F. Zhang, Y. Zhao, S. Tong, B. Han and Z. Liu, *CCS Chemistry*, 2023, **5**, 1854-1865.
18. F. A. Rahimi, S. Dey, P. Verma and T. K. Maji, *ACS Catalysis*, 2023, **13**, 5969-5978.
19. F. Meng, J. Wang, M. Chen, Z. Wang, G. Bai and X. Lan, *ACS Catalysis*, 2023, **13**, 12142-12152.
20. Z. Fu, X. Wang, A. M. Gardner, X. Wang, S. Y. Chong, G. Neri, A. J. Cowan, L. Liu, X. Li and A. Vogel, *Chemical Science*, 2020, **11**, 543-550.
21. H. Zhang, J. Wei, J. Dong, G. Liu, L. Shi, P. An, G. Zhao, J. Kong, X. Wang and X. Meng, *Angewandte Chemie*, 2016, **128**, 14522-14526.
22. R. Xu, X.-S. Wang, H. Zhao, H. Lin, Y.-B. Huang and R. Cao, *Catalysis Science & Technology*, 2018, **8**, 2224-2230.
23. H.-P. Liang, A. Acharjya, D. A. Anito, S. Vogl, T.-X. Wang, A. Thomas and B.-H. Han, *ACS Catalysis*, 2019, **9**, 3959-3968.
24. X. Chen, Q. Dang, R. Sa, L. Li, L. Li, J. Bi, Z. Zhang, J. Long, Y. Yu and Z. Zou, *Chemical Science*, 2020, **11**, 6915-6922.
25. R. Paul, R. Das, N. Das, S. Chakraborty, C. W. Pao, Q. Thang Trinh, G. K. Kalhara Gunasooriya, J. Mondal and S. C. Peter, *Angewandte Chemie International Edition*, 2023, **62**, e202311304.